Generalized Scattering Matrix of Generalized Two-Port Discontinuities: Application to Four-Port and Nonsymmetric Six-Port Couplers

Jaime Esteban and Jesús M. Rebollar

Abstract—**A field theory analysis of multiport, multidiscontinuity structures based on the generalized scattering matrix of a generalized two-port discontinuity concept is presented. The analysis can be used in any structure equipped with any number of input and output ports, and results in substantial simplifications over previous analyses. The GSM's of generalized two-port discontinuities can also be cascaded with the same procedure as the two-port discontinuities and can be used to determine the electromagnetic field and the Poynting vector at every point of the structure. The GSM of the generalized two-port technique is used to analyze four-port and nonsymmetric six-port branch-waveguide directional couplers, and good agreement between the theoretical results and experimental data is obtained.**

I. Introduction

WAVEGUIDE structures with two ports and a large number of discontinuities are widely used in integrated microwave and millimeter-wave circuits, in applicators for medical applications, and in satellite communication systems. For instance, they are used in all-metal-insert filters [1], dual-band dual-mode inwate (integrated waveguide technology) filters [2], coaxial filters [3], corrugated polarizers [4], multistep waveguide applicators [5], rectangular and conical corrugated horns [6], [7], mode converters [8], tapers [9], and phase shifters [10].

A very powerful and accurate technique for analyzing most of these structures is based on modal analysis [11], [12] and on the generalized scattering matrix (GSM) concept of discontinuities [13], [14]. This technique takes into account the local effect of and the interactions between higher order modes at and between discontinuities. There are a large number of waveguide structures with more than two ports and a large number of discontinuities, for example, directional couplers [15], [16], waveguide array applicators [17], multiplexers [18], [19], mode transducers [20], and mode converters [21].

Manuscript received November 29, 1990 revised May 14, 1991. This work was supported by the Comisión Interministerial de Ciencia y Tecnologia (CICYT).

The authors are with the Grupo de Electromagnetismo Aplicado y Microondas, E.T.S.I. Telecomunicación, Universidad Politécnica de Madrid, Ciudad Universitaria, 28040 Madrid, Spain.

IEEE Log Number 9102333.

A generalization of the GSM concept for N-furcated waveguide discontinuities, i.e., $N+1$ ports, has been proposed by Mansour and MacPhie [22]. Such a generalization is of great interest for the analysis of multiport, multidiscontinuity structures. If the multiport discontinuity is regarded as a generalized two-port discontinuity, some important simplifications in the analysis of multiport, multidiscontinuity structures can be made [23].

In this paper, the GSM of the generalized two-port discontinuity concept is applied to the analysis of four-port directional couplers. As a new application of this technique, nonsymmetric six-port directional couplers are also considered.

Some applications of these devices, for instance, in beam-forming networks (BFN's) of spacecraft antennas, require knowledge of the electromagnetic (EM) field distribution in the structure. The technique considered in this paper can determine the EM field and Poynting vector distributions in the structure, thus proving its great potential. Several examples of electric field and Poynting vector distributions are presented.

II. GSM of a Generalized Two-Port Discontinuity

In order to solve multidiscontinuity geometries with more than two ports, the first step is to obtain the GSM of a generalized N-furcated waveguide discontinuity in a very simple form and without any restriction. The theoretical treatment of this problem has been fully described in [23]. However, the main aspects will be discussed here because some background on the formulation is needed for a) the derivation of the modal amplitudes in the different regions of the structure (Section III) and b) the derivation of the GSM of the generalized two-port for a composite discontinuity that allows a new and rigorous analysis technique for nonsymmetric six-port couplers (Section V).

A general N-furcated waveguide discontinuity is presented in Fig. 1(a). This discontinuity has $N+1$ ports, so its GSM requires $(N+1)\times(N+1)$ matrices $[S_{mn}]$ for its

0018-9480/91/1000-1725$01.00 ©1991 IEEE

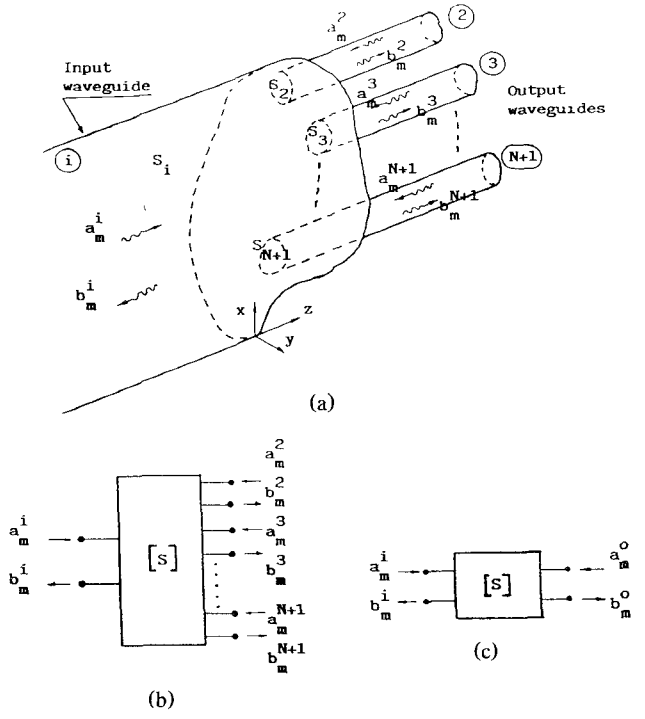

Fig. 1. Waveguide discontinuity: (a) N-furcated waveguide discontinuity; (b) generalized scattering matrix (GSM) of an N-furcated waveguide discontinuity; (c) GSM of a generalized two-port discontinuity.

total characterization. The GSM can be obtained by means of modal analysis, as has been suggested in [11]–[14].

Considering the boundary conditions for the transverse electric and magnetic fields at the N-furcated waveguide in a way similar to that proposed by Mansour and MacPhie [22], and after some algebraic manipulation, the GSM of the generalized two-port discontinuity (corresponding to Fig. 1(c)) can be written as

$$\begin{bmatrix} [B_i] \\ [B_o] \end{bmatrix} = \begin{bmatrix} [S_{ii}] & [S_{io}] \\ [S_{oi}] & [S_{oo}] \end{bmatrix} \begin{bmatrix} [A_i] \\ [A_o] \end{bmatrix}. \tag{1}$$

Equation (1) indicates that an N-furcated waveguide can be treated as a generalized two-port discontinuity, and its four block matrices constitute the GSM of the generalized two-port.

If the column matrices $[A_o]$ and $[B_o]$ are partitioned into the N column matrices corresponding to the amplitudes of the incident and reflected modes of the N output waveguides, the GSM can be written as (see Fig. 1(b))

$$\begin{bmatrix} [B_1] \\ \hline [B_2] \\ [B_3] \\ \vdots \\ [B_{N+1}] \end{bmatrix} = \left[\begin{array}{c|ccccc} [S_{11}] & [S_{12}] & [S_{13}] & \cdots & [S_{N+1\,1}] \\ \hline [S_{21}] & [S_{22}] & [S_{23}] & \cdots & [S_{N+1\,2}] \\ [S_{31}] & [S_{32}] & [S_{33}] & \cdots & [S_{N+1\,3}] \\ \vdots & \vdots & \vdots & \ddots & \vdots \\ [S_{N+1\,1}] & [S_{N+1\,2}] & [S_{N+1\,3}] & \cdots & [S_{N+1\,N+1}] \end{array}\right] \begin{bmatrix} [A_1] \\ \hline [A_2] \\ [A_3] \\ \vdots \\ [A_{N+1}] \end{bmatrix}. \tag{2}$$

Although the GSM's of (1) and (2) are similar, (2) illustrates the physics of the discontinuity in a better manner than (1). However, the GSM of the generalized two-port, i.e., (1), is more general, and the four matrices

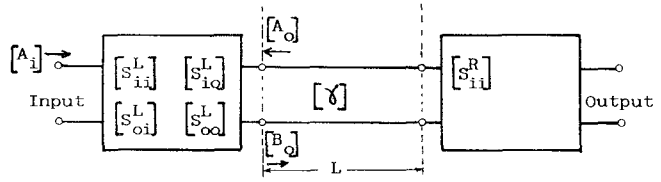

Fig. 2. Waveguide or multiwaveguide section of length L embedded between the two-port GSM's of the substructures existing to the left and right of the section considered.

that constitute it are derived using the same algebraic manipulations as in the case of the two-port discontinuity [23]. This results in an important algebraic simplification. Furthermore, these four matrices can be divided into $(N+1)\times(N+1)$ matrices using (1) and (2), if necessary.

Once the GSM's of the generalized two-port discontinuities are known, they can be linked together in two different ways: by means of either their outputs (N ports) with N waveguide sections of length L or their inputs (one port) with one waveguide section of length L. Both cases are considered in a similar form [23], and can be cascaded using a procedure similar to the one proposed in [24] for two-port discontinuities.

III. Electric Field and Poynting Vector Computation

The GSM of the generalized two-port discontinuity concept can be used to compute the electric and magnetic fields and the Poynting vector at every point of the structure.

The amplitudes of the propagating and nonpropagating modes under consideration in the $\pm \hat{z}$ directions (a_m^j, b_m^j) in the jth waveguide or multiwaveguide section linking two adjacent multiport discontinuities are obtained from

1) the column vector $[A_i]$ of the amplitudes corresponding to the modes which impinge on the input port of the structure;
2) the GSM of the generalized two-port discontinuity $[S^L]$ of the existing substructure between the input port and the discontinuity placed at the left of the section considered; and
3) the reflection matrix $[S_{ii}^R]$ of the existing substructure to the right of the section considered (Fig. 2).

The matrices $[S^L]$ and $[S_{ii}^R]$ are calculated from the GSM's of the different multiport discontinuities that compose the whole structure by means of the procedure mentioned in Section II.

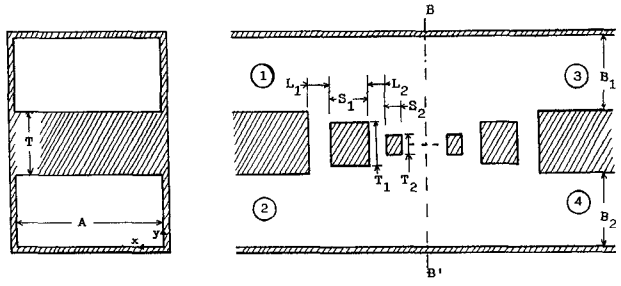

Fig. 3. Four-port branch waveguide directional coupler.

The column matrices with the amplitudes of the modes, $[A_o]$ and $[B_o]$, are calculated as follows:

$$[B_o] = \left([U] - [S_{oo}^L][\gamma][S_{ii}^R][\gamma]\right)^{-1}[S_{oi}^L][A_i]$$

$$[A_o] = [\gamma][S_{ii}^R][\gamma][B_o] \tag{3}$$

where $[U]$ is the unit matrix. The quantity $[\gamma]$ is a diagonal matrix with elements $\exp(-\gamma_m^j L)$, where γ_m^j is the propagation constant of the mth mode of the jth waveguide.

Once these amplitudes are known, the EM field is easily computed by means of its expression in terms of the electric and magnetic fields of the section's eigenmodes.

It should be noted that when the linking section consists of two or more waveguides, the computed $[A_o]$ and $[B_o]$ column vectors must be partitioned into the different column vectors corresponding to the modal amplitudes of the different waveguides. In this case the matrix $[\gamma]$ consists of different block diagonal matrices [23].

Once the electric and magnetic fields are obtained, the Poynting vector is calculated in a straightforward manner.

IV. Four-Port Branch-Waveguide Directional Coupler

In this section, the GSM of the generalized two-port concept is applied to the analysis of a four-port branch-waveguide directional coupler (four-port BWDC). The geometry of the structure is well known and is schematically shown in Fig. 3.

Different methods have been applied to the analysis of this structure:

a) With the transmission line model, either equivalent circuits are used to simulate the E-plane T junctions [25] or an accurate characterization of this junction is obtained from a cavity field expansion [26]. Even in this second case, the transmission line model does not take into account, in an adequate manner, all the higher order mode interactions, and discrepancies between experimental data and numerical predictions have been observed.

b) Field theory analysis uses both the mode matching technique and the admittance matrix formulation [16]. This technique overcomes the difficulties mentioned above, for it considers all parasitic phenomena associated with higher order modes. Because of symmetry considerations, the four-port structure can be reduced to the analysis of two structures with only two ports. However, nonsymmetric structures cannot be easily analyzed with this formulation.

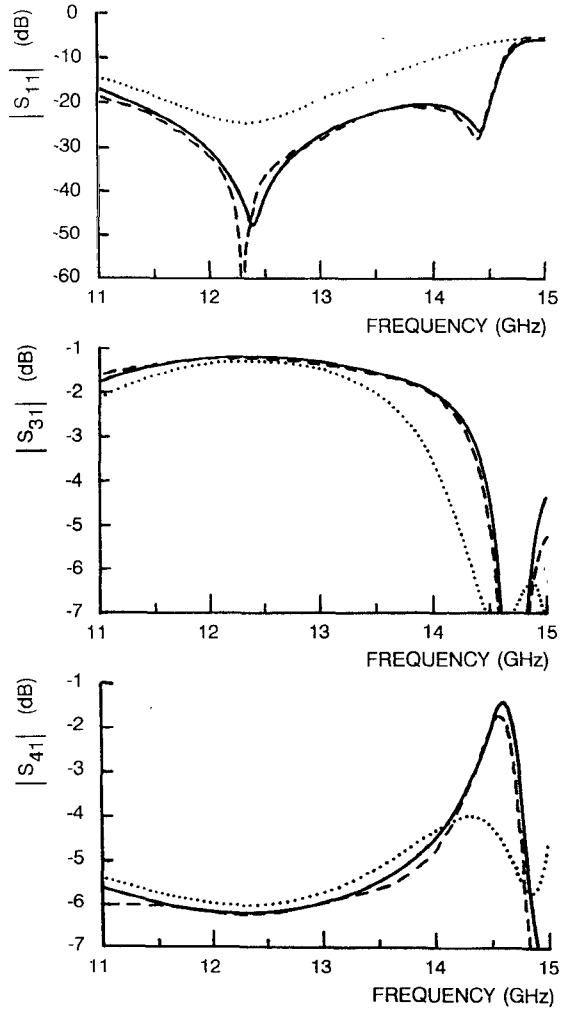

Fig. 4. Two-branch four-port coupler (dimensions in mm: $A = 19.05$, $B1 = B2 = 9.525$, $T = 7.182$, $L1 = 7.852$, $S1 = 1.179$, $T1 = 3.680$). Experimental results (dashed lines). Results computed by means of the GSM of the generalized two-port concept (solid lines). Results computed by means of the connected T-junction model (dotted lines).

The GSM of the generalized two-port concept described in Section II is a field theory analysis which uses the mode matching technique, considers all effects of higher order mode interactions, and can be applied without restrictions to nonsymmetric structures.

The four-port BWDC is assumed to consist of a combination of one basic discontinuity, i.e., a bifurcation in the E plane of the rectangular waveguide. The GSM of this discontinuity is a particular case of that mentioned in the previous section with $N = 2$. In this case, we consider a TE_{m0} wave incident on one of the three ports of the discontinuity, which is uniform in the x direction, so that the TE_{mn}^x family of modes will be excited [27].

The number of modes employed in each section of the BWDC is proportional to its height in order to achieve a high convergence rate while obtaining accurate results.

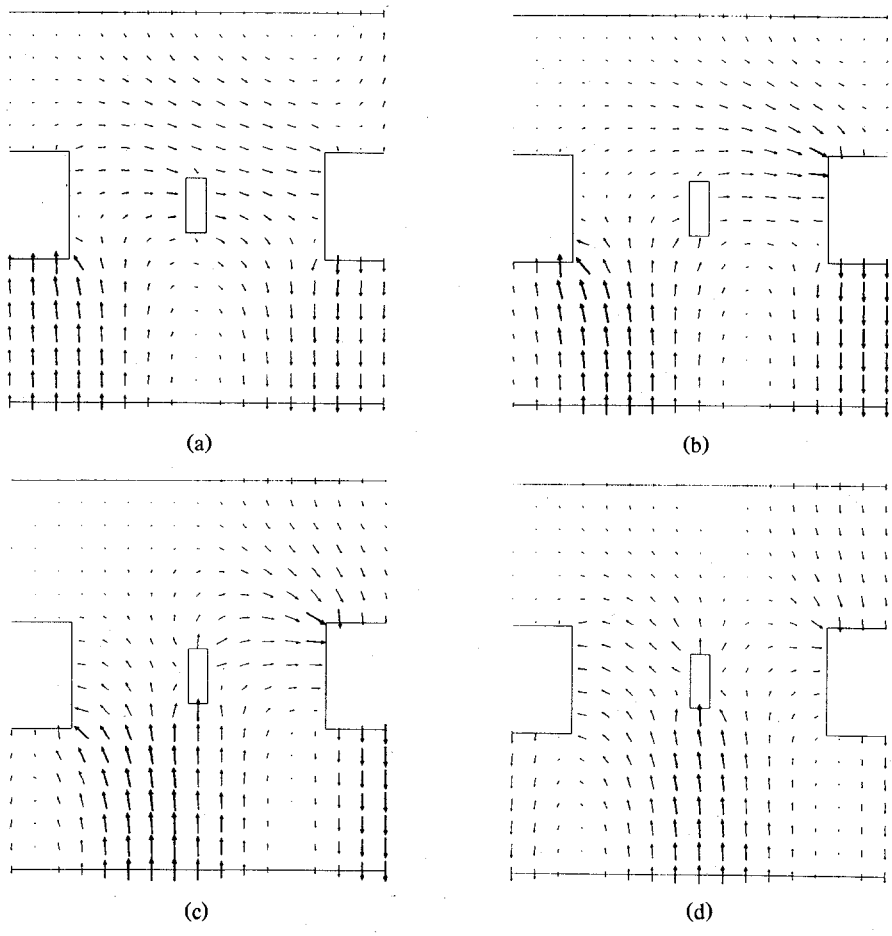

Fig. 5. Electric field distribution in the two-branch four-port BWDC with dimensions presented in Fig. 4 in the middle plane $x = A/2$ at frequency $f = 12.3$ GHz and at different times: (a) $t = t_0$, (b) $t = t_0 + T/12$, (c) $t = t_0 + T/6$, (d) $t = t_0 + T/4$.

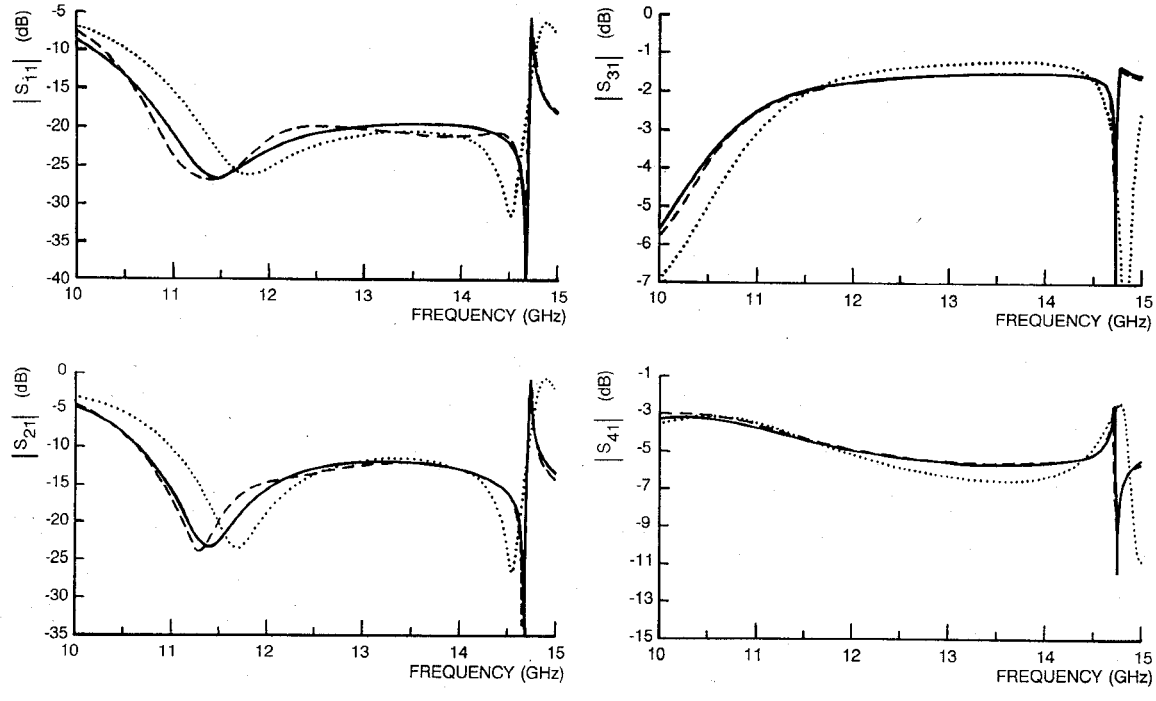

Fig. 6. Three-branch four-port coupler (dimensions in mm: $A = 19.05$, $B1 = B2 = 9.525$, $T = 6.65$, $L1 = 4.13$, $S1 = 1.59$, $T1 = 2.99$, $L2 = 10.75$). Experimental results (dashed lines). Results computed by means of the GSM of the generalized two-port concept (solid lines). Results computed by means of the connected T-junction model (dotted lines).

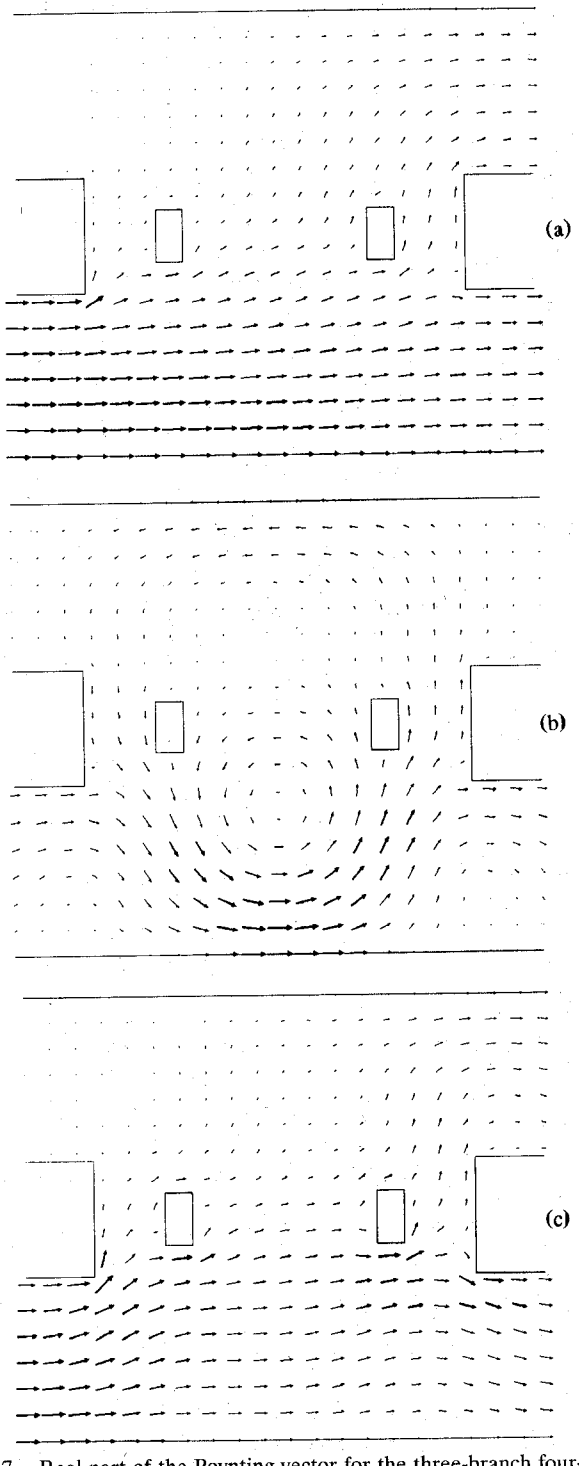

Fig. 7. Real part of the Poynting vector for the three-branch four-port BWDC with dimensions presented in Fig. 6 at three different frequencies: (a) $f = 11.5$ GHz, (b) $f = 14.75$ GHz, and (c) $f = 15.5$ GHz.

Typically, 12 modes are considered in the highest cross section. Calculations have also been performed with up to 30 modes to verify the accuracy of the results.

In Fig. 4, the computed responses of a two-branch coupler are compared with measurements. This figure indicates that the theoretical responses computed by means of the GSM of the generalized two-port concept (solid lines) are in excellent agreement with experimental

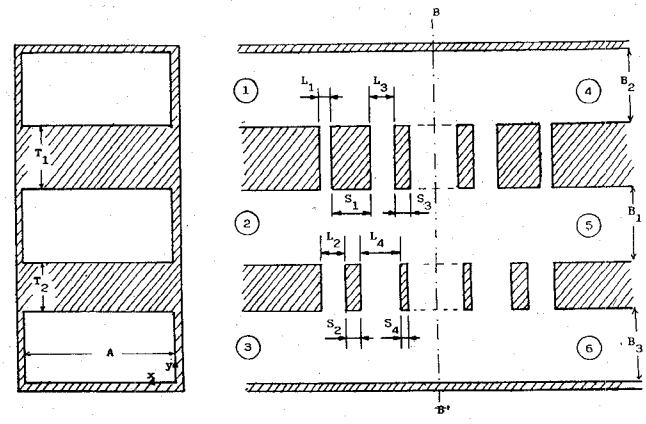

Fig. 8. Nonsymmetric six-port coupler.

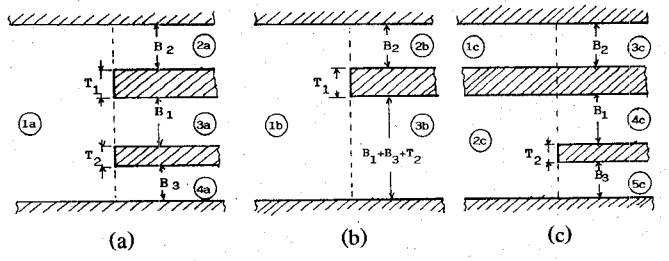

Fig. 9. Basic multiport discontinuities of a six-port coupler. (a) Trifurcation in E plane of rectangular waveguide. (b) Bifurcation in E plane of rectangular waveguide. (c) Composite discontinuity with two isolated input ports, one directly linked to one of the output ports and the other bifurcated into two output ports.

measurements (dashed lines). The GSM and experimental results are also compared in Fig. 4 with those obtained by means of an accurate analysis of T junctions [26] connected through the equivalent transmission line of a rectangular waveguide excited only by the TE_{10} mode (dotted lines), and significant differences between experimental data and the results of this technique are observed.

The electric field in the four-port BWDC considered above has been calculated by means of the procedure described in Section III, and is presented in Fig. 5, which illustrates the electric field in the middle plane $x = A/2$ at a frequency of 12.3 GHz at different times.

Fig. 5 clearly illustrates the reduced dimensions of the central post of this narrow-band coupler. These reduced dimensions imply a significant higher order mode interaction between T junctions, which can explain the discrepancies between experimental data and the computed results based on the use of T junctions connected through the equivalent line of the fundamental mode (dashed and dotted lines in Fig. 4). In fact, as can be observed in Fig. 5, the computed electric field in the connecting sections between T junctions can hardly be described by only the fundamental mode of the rectangular waveguides that constitute those sections.

The computed and measured responses of a three-branch coupler are presented in Fig. 6. In comparison with the theory involving connected T junctions, the method based on the GSM of the generalized two-port is

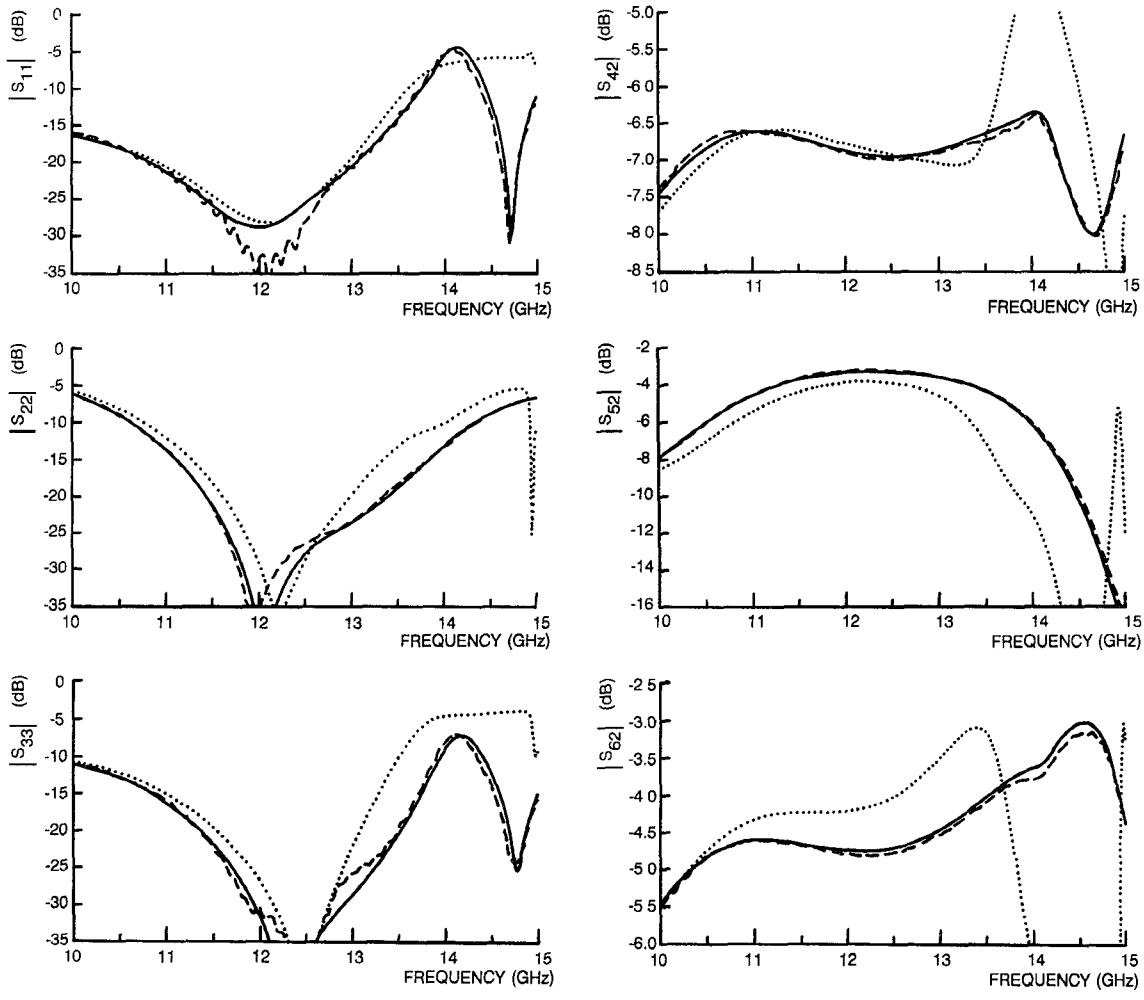

Fig. 10. Three-branch nonsymmetric SPC (dimensions in mm: $A = 19.05$, $B1 = B2 = 9.525$, $T1 = 6.905$, $T2 = 7.261$, $L1 = 2.794$, $L2 = 3.883$, $L3 = 5.769$, $L4 = 7.947$, $S1 = 3.413$, $S2 = 1.235$). Experimental results (dashed lines). Results computed by means of the GSM of the generalized two-port concept (solid lines). Results computed by means of the connected single and double T-junction model (dotted lines).

able to predict more accurately the reflection and coupling levels. The resonance phenomenon which occurs at the frequency of 14.75 GHz is also predicted more accurately by the GSM technique.

The real part of the Poynting vector in the middle plane $x = A/2$ at several frequencies is presented in Fig. 7 for the three-branch four-port BWDC above described. It is shown in Fig. 7 that the energy flows mainly through the second and third branches, whereas very little energy flows through the first branch of the structure (Fig. 7(a), $f = 11.5$ GHz).

In Fig. 7(b) which corresponds to a frequency of 14.75 GHz, a vortex in the Poynting vector centered under the second branch can be observed. In this region, constituted by a rectangular waveguide of dimensions 19.05×25.7 mm, the TE_{11}^x and TE_{12}^x modes are propagating. These higher order modes provide the transverse power flow required for the vortex formation. A similar phenomenon has been observed in rectangular waveguides with an iris [28]. It is worth noting that there is a correlation between this vortex and the sharp peak of the structure response presented in Fig. 6 at the same frequency. At a higher frequency ($f = 15.5$ GHz, Fig. 7(c)) the Poynting vector exhibits a similar behavior to that presented at a frequency $f = 11.5$ GHz.

As illustrated above, the Poynting vector representation can be used to determine the regions in which high power densities occur and to give a deeper insight into resonance phenomena.

V. Nonsymmetric Six-Port Branch-Waveguide Directional Coupler

A more complex structure, one where the GSM of the generalized two-port shows its great potential, is the nonsymmetric six-port branch coupler (SPC) presented in Fig. 8.

This structure is of great interest for applications in power divider networks (PDN's) for contoured beam satellite antennas, for it minimizes the number of required power dividers in the PDN, thus reducing the length of the signal paths and minimizing losses, volume, and weight.

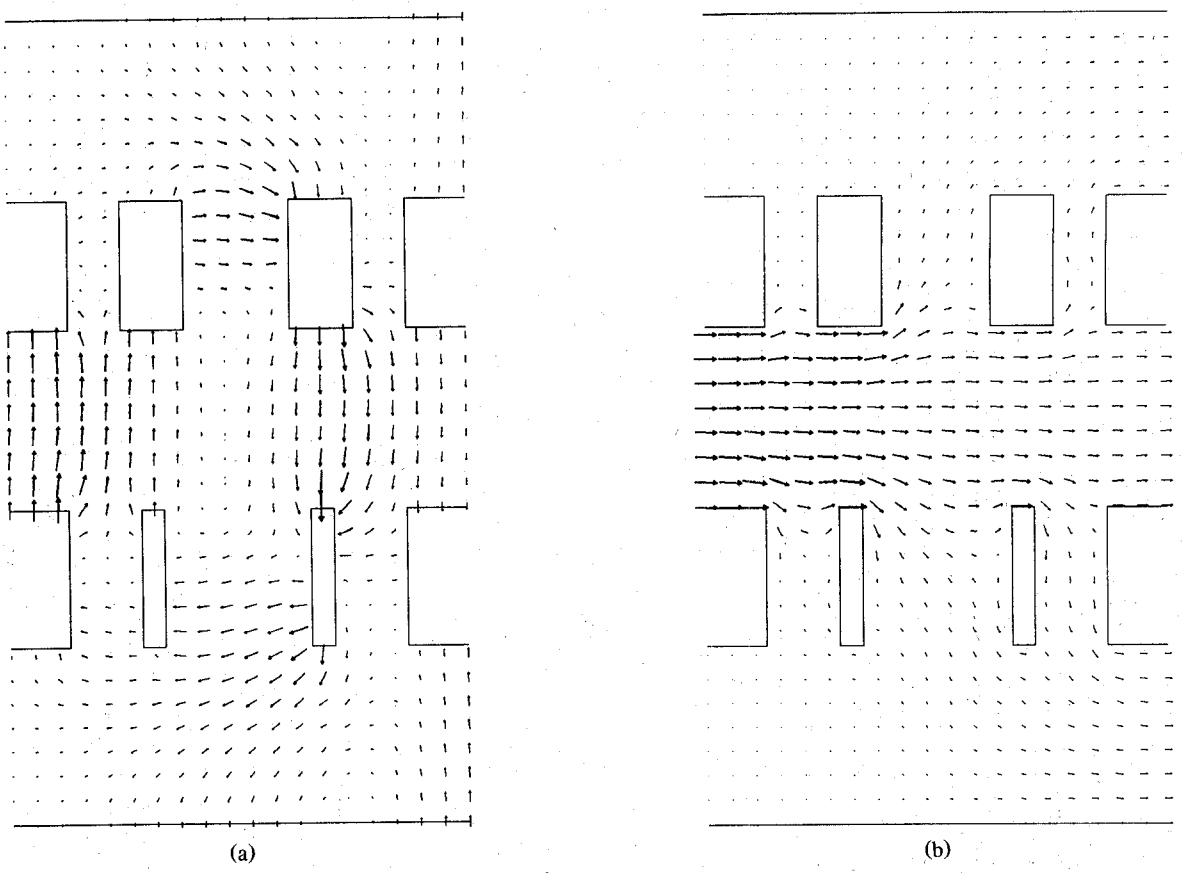

Fig. 11. Electric field and Poynting vector in the middle plane $x = A/2$ of the nonsymmetric SPC with dimensions presented in Fig. 10 at $f = 12.3$ GHz. Structure excited by the fundamental mode in the central input port 2. (a) Electric field ($t = 0$). (b) Real part of the Poynting vector.

The first SPC was proposed by Kühn *et al.* [29]. In that work, owing to the symmetry of the structure, two of the three output power levels into which the input power was split were equal. This severe restriction reduces the applicability of the symmetric SPC. In order to obtain arbitrary power ratios in the three output ports, a nonsymmetric SPC was proposed by Carle [30] using a technique that results in an accurate analysis of double asymmetrical E-plane T junctions. However, Carle [30] analyzed the overall structure as a set of different single and double asymmetrical E-plane T junctions connected through transmission lines. Therefore, interaction effects of higher order modes were not taken into account in these connections. For this reason, differences greater than 0.5 dB in the coupling values can be observed between the numerical and experimental results.

In this section, the nonsymmetric SPC is analyzed by means of the GSM of the generalized two-port concept in order to consider all the higher order mode interactions and obtain more accurate results.

The nonsymmetric SPC is assumed to consist of cascaded multiport discontinuities that can be classified into three basic groups:

a) trifurcation in the E plane of the rectangular waveguide (Fig. 9(a));
b) bifurcation (Fig. 9(b));
c) composite discontinuity with two isolated input ports, one directly linked to one of the output ports and the other bifurcated into two output ports (Fig. 9(c)). This discontinuity is not as simple as the N-furcation presented in Section II. The derivation of the GSM of the generalized two-port for this composite discontinuity is presented in the Appendix.

The same general considerations about the family and number of modes to be employed in these basic discontinuities as those for the case of bifurcation described in Section IV apply here.

In Fig. 10, numerical and experimental results for a three-branch nonsymmetric SPC are presented. Again, an excellent agreement between experimental data (dashed lines) and numerical results obtained by means of the GSM of the generalized two-port discontinuity concept (solid lines) can be observed. For comparison, the results obtained by the authors using a procedure similar to that proposed in [30] are also included in the figure (dotted lines). As stated before, significant differences are observed between this theory and experimental data.

For both the four-port and the six-port couplers, it is worth noting that, in the useful band of the couplers (where the reflection and isolation levels are low enough), the differences between measured coupling levels and the

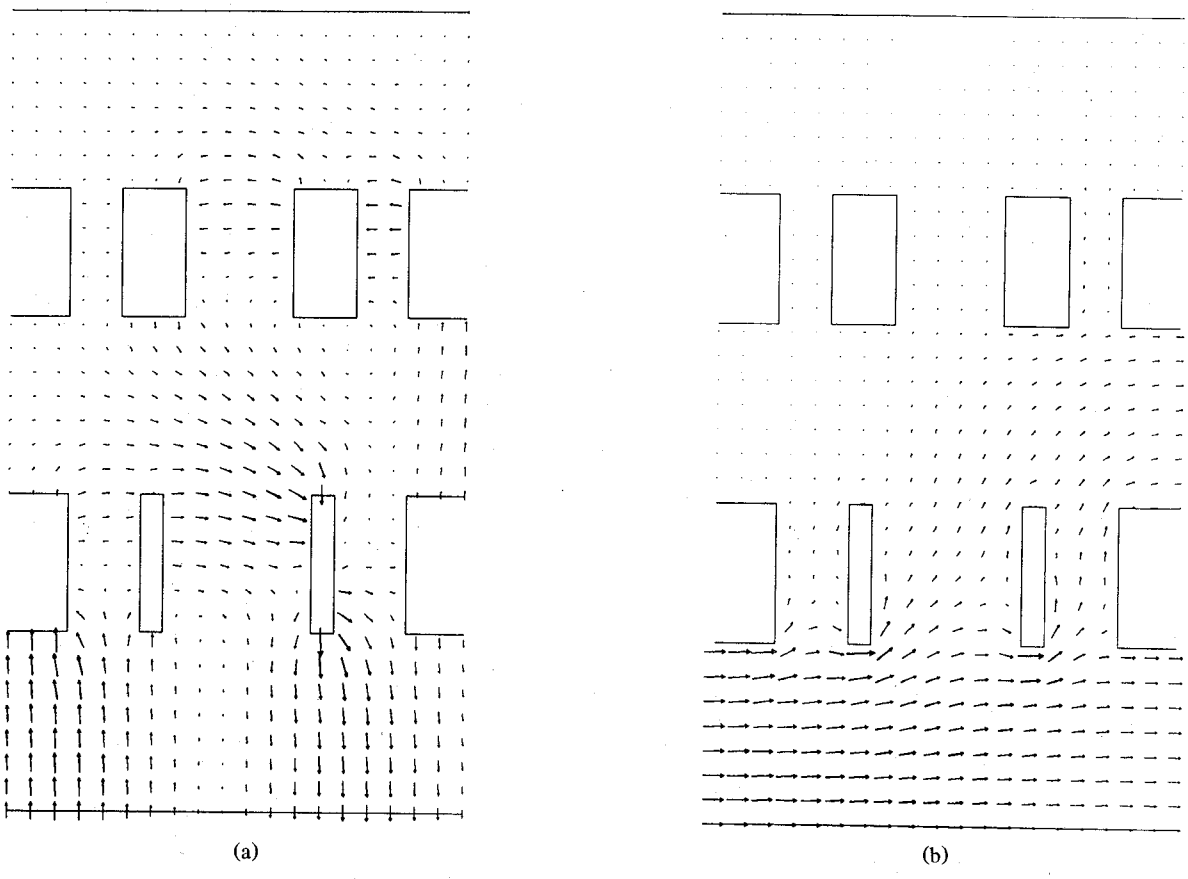

Fig. 12. Electric field and Poynting vector in the middle plane $x = A/2$ of the nonsymmetric SPC with dimensions presented in Fig. 10 at $f = 12.3$ GHz. Structure excited by the fundamental mode in the lower input port 3. (a) Electric field ($t = 0$). (b) Real part of the Poynting vector.

coupling levels predicted by the connected T-junction model are lower. However, even in these frequency bands, unacceptable differences are obtained (see Figs. 4, 6, and 10).

The electric field and the Poynting vector in the middle plane $x = A/2$ at a frequency of 12.3 GHz for the structure considered in Fig. 10 are presented in Fig. 11. The fundamental mode TE_{10} is considered as the input field at the central input port (port 2). In Fig. 12, the electric field and the Poynting vector of the same structure considering the fundamental mode TE_{10} incident on port 3 are presented.

The electric field and the Poynting vector shown in Figs. 11 and 12 are of great importance in determining regions of high field intensities and for the prevention of multipactor breakdown phenomena [31].

VI. Conclusions

A field theory analysis of multiport, multidiscontinuity structures has been presented. An extension of the well-known generalized scattering matrix (GSM) technique for structures with two-port multidiscontinuities has been proposed to analyze with high accuracy multiport, multidiscontinuity structures. The proposed extension is based on the GSM of the generalized two-port discontinuity concept. Very important simplifications in the analysis of these structures can be obtained, because the technique is independent of the number of ports and because complex structures can be analyzed by cascading, using a simple procedure similar to that applied to structures with only two ports.

To illustrate the features of the proposed formulation and to demonstrate its effectiveness, four-port and nonsymmetric six-port branch waveguide directional couplers have been analyzed. An excellent agreement between numerical predictions and experimental data has been obtained.

The response of the analyzed couplers has also been obtained by means of the analysis of single and double T junctions connected through transmission lines. This analysis yields significant discrepancies with measurements because it neglects higher order mode interactions between adjacent single and double T junctions.

The GSM of the generalized two-port discontinuity concept has been used to calculate the local electric and magnetic fields and the Poynting vector, which are of great interest in determining regions of high field intensity.

Appendix

In order to obtain the GSM of the generalized two-port $[S^c]$ of the multiport discontinuity of Fig. 9(c), it is more convenient to begin with the five-port scattering matrix of

the discontinuity, written as

$$\begin{bmatrix} [B_1] \\ [B_2] \\ \hline [B_3] \\ [B_4] \\ [B_5] \end{bmatrix} = \left[\begin{array}{cc|ccc} [S^c_{11}] & [S^c_{12}] & [S^c_{13}] & [S^c_{14}] & [S^c_{15}] \\ [S^c_{21}] & [S^c_{22}] & [S^c_{23}] & [S^c_{24}] & [S^c_{25}] \\ \hline [S^c_{31}] & [S^c_{32}] & [S^c_{33}] & [S^c_{34}] & [S^c_{35}] \\ [S^c_{41}] & [S^c_{42}] & [S^c_{43}] & [S^c_{44}] & [S^c_{45}] \\ [S^c_{51}] & [S^c_{52}] & [S^c_{53}] & [S^c_{54}] & [S^c_{55}] \end{array}\right] \begin{bmatrix} [A_1] \\ [A_2] \\ \hline [A_3] \\ [A_4] \\ [A_5] \end{bmatrix}. \quad \text{(A1)}$$

Since ports 1c and 3c are isolated from ports 2c, 4c, and 5c by the metallic E plane of thickness T_1, the matrices involving coupling between these ports must be null, i.e.,

$$[S^c_{mn}] = [0] \quad \text{for } m = 1,3 \text{ and } n = 2,4,5$$
$$m = 2,4,5 \text{ and } n = 1,3 \quad \text{(A2)}$$

where [0] is the null matrix

Since ports 1c and 3c are directly connected without any discontinuity, all the incident modes are transmitted with the same magnitude and phase, and no reflection occurs on these ports, i.e.,

$$[S^c_{31}] = [S^c_{13}] = [U]$$
$$[S^c_{11}] = [S^c_{33}] = [0]. \quad \text{(A3)}$$

The other matrices, $[S^c_{mn}]$ $(m, n = 2,4,5)$, are obtained by calculating the GSM of the generalized two-port of the bifurcation at port 2c into ports 4c and 5c as in previous cases and partitioning according to (2) as

$$\begin{bmatrix} [B_2] \\ \hline [B_4] \\ [B_5] \end{bmatrix} = \left[\begin{array}{c|cc} [S^c_{22}] & [S^c_{24}] & [S^c_{25}] \\ \hline [S^c_{42}] & [S^c_{44}] & [S^c_{45}] \\ [S^c_{52}] & [S^c_{54}] & [S^c_{55}] \end{array}\right] \begin{bmatrix} [A_2] \\ \hline [A_4] \\ [A_5] \end{bmatrix}. \quad \text{(A4)}$$

Finally, the GSM $[S^c]$ of (A1) can be constructed using (A2)–(A4) as

$$[S^c] = \left[\begin{array}{c|c} [S^c_{ii}] & [S^c_{io}] \\ \hline [S^c_{oi}] & [S^c_{oo}] \end{array}\right] = \left[\begin{array}{cc|ccc} [0] & [0] & [U] & [0] & [0] \\ [0] & [S^c_{22}] & [0] & [S^c_{24}] & [S^c_{25}] \\ \hline [U] & [0] & [0] & [0] & [0] \\ [0] & [S^c_{42}] & [0] & [S^c_{44}] & [S^c_{45}] \\ [0] & [S^c_{52}] & [0] & [S^c_{54}] & [S^c_{55}] \end{array}\right]. \quad \text{(A5)}$$

Acknowledgment

The authors are grateful to CASA-División Espacio, Madrid, Spain, for allowing them to reproduce their experimental results.

References

[1] R. Vahldieck, J. Bornemann, F. Arndt, and D. Grauerholz, "Optimized waveguide E-plane metal insert filters for millimeter-wave applications," *IEEE Trans. Microwave Theory Tech.*, vol. MTT-31, pp. 65–69, Jan. 1983.

[2] F. Henze, J. Modelski, and J. H. Hinken, "Investigations of the temperature sensitivity of dual-band dual-mode inwate filters for satellite converters," in *Proc. 18th European Microwave Conf.*, Sept. 1988, pp. 956–961.

[3] R. Levy and T. E. Rozzi, "Precise design of coaxial low-pass filters," *IEEE Trans. Microwave Theory Tech.*, vol. MTT-16, pp. 142–147, Mar. 1968.

[4] U. Tucholke, F. Arndt, and T. Wriedt, "Field theory design of square waveguide iris polarizers," *IEEE Trans. Microwave Theory Tech.*, vol. 36, pp. 156–160, Jan. 1986.

[5] J. M. Rebollar and J. A. Encinar, "Design and optimization of multi-stepped waveguide applicators for medical applications," *J. Microwave Power*, vol. 19, pp. 259–267, 1984.

[6] E. Kühn and V. Hombach, "Computer aided analysis of corrugated horns with axial or ring-loaded radial slots," in *Proc. Int. Conf. Antennas Propagat.*, 1983, pp. 127–131.

[7] J. A. Encinar and J. M. Rebollar, "A hybrid technique for analyzing corrugated and non-corrugated rectangular horns," *IEEE Trans. Antennas Propagat.*, vol. AP34, pp. 961–969, Aug. 1986.

[8] M. Thumm, "Computer-aided analysis and design of corrugated TE11 to HE11 mode converters in highly overmoded waveguides," *Int. J. Infrared and Millimeter Waves*, vol. 6, no. 7, pp. 577–597, 1985.

[9] H. Flügel and E. Kühn, "Computer-aided design of circular waveguide tapers," *IEEE Trans. Microwave Theory Tech.*, vol. 36, pp. 332–336, Feb. 1988.

[10] J. Dittloff, F. Arndt, and D. Grauerholz, "Optimum design of waveguide E-plane stub-loaded phase shifters," *IEEE Trans. Microwave Theory Tech.*, vol. 36, pp. 582–587, Mar. 1988.

[11] A. Wexler, "Solution of waveguide discontinuities by modal analysis," *IEEE Trans. Microwave Theory Tech.*, vol. MTT-15, pp. 508–517, Sept. 1967.

[12] P. H. Mastermann and P. J. B. Clarricoats, "Computer field-matching solution of waveguide transverse discontinuities," *Proc. Inst. Elec. Eng.*, vol. 118, pp. 51–63, 1971.

[13] R. Mittra and S. W. Lee, *Analytic Techniques in the Theory of Guided Waves*. New York: Macmillan, 1971.

[14] T. Itoh, *Numerical Techniques for Microwave and Millimeter Wave Passive Structures*. New York: Wiley, 1989, ch. 10.

[15] H. Schmiedel and F. Arndt, "Field theory of rectangular waveguide multiple-slot narrow wall couplers," *IEEE Trans. Microwave Theory Tech.*, vol. MTT-34, pp. 791–798, July 1986.

[16] F. Alessandri, G. Bartolucci, and R. Sorrentino, "Admittance matrix formulation of waveguide discontinuity problems: Computer-aided design of branch guide directional couplers," *IEEE Trans. Microwave Theory Tech.*, vol. 36, pp. 394–403, Feb. 1988.

[17] Y. Nikawa, T. Kitsumata, M. Kikuchi, and S. Mori, "An electric field converging applicator with heating pattern controller for microwave hyperthermia," *IEEE Trans. Microwave Theory Tech.*, vol. MTT-34, pp. 631–636, May 1986.

[18] Y. C. Shih, L. Q. Bui, and T. Itoh, "Millimeter-wave diplexers with printed elements," *IEEE Trans. Microwave Theory Tech.*, vol. MTT-33, pp. 1465–1469, Dec. 1985.

[19] R. Vahldieck and B. Varailhon de la Filolie, "A novel waveguide quadruplexer for millimeter wave applications," in *Proc. 19th European Microwave Conf.*, Sept. 1989, pp. 621–626.

[20] H. Schmiedel and F. Arndt, "Mode transducer utilizing asymmetric waveguide narrow wall coupling," in *Proc. 15th European Microwave Conf.*, Sept. 1985, pp. 737–742.

[21] H. W. Schilling and R. E. Collin, "Circular waveguide bifurcation for asymmetric modes," *Proc. Inst. Elec. Eng.*, vol. 131, pt. H, pp. 397–404, Dec. 1984.

[22] R. R. Mansour and R. H. MacPhie, "Scattering at N-furcated parallel-plate waveguide junction," *IEEE Trans. Microwave Theory Tech.*, vol. MTT-33, pp. 830–835, Sept. 1985.

[23] J. M. Rebollar and J. A. Encinar, "Field theory analysis of multiport-multidiscontinuity structures: Application to short-circuited E-plane septum," *Proc. Inst. Elec. Eng.*, vol. 135, pt. H, no. 1, pp. 1–7, Feb. 1988.

[24] H. Patzelt and F. Arndt, "Double-plane steps in rectangular waveguides and their application for transformers, irises and filters," *IEEE Trans. Microwave Theory Tech.*, vol. MTT-30, pp. 771–776, May 1982.
[25] G. L. Mathaei, L. Young, and E. M. T. Jones, *Microwave Filters, Impedance Matching Networks and Coupling Structures*. New York: McGraw-Hill, 1964.
[26] E. Kühn, "Improved design and resulting performance of multiple branch-waveguide directional couplers," *Arch. Elek. Übertragung.*, vol. 28, pp. 206–214, 1974.
[27] R. E. Collin, *Field Theory of Guided Waves*. New York: McGraw-Hill, 1960, pp. 22–27, 338–359, 447–449.
[28] R. W. Ziolkowski and J. B. Grant, "Vortex formation near iris in a rectangular waveguide," *IEEE Trans. Microwave Theory Tech.*, vol. 36, pp. 1164–1182, Nov. 1988.
[29] E. Kühn, H. Schmiedel, and R. Waugh, "Six-port branch-waveguide directional couplers," in *Proc. 16th European Microwave Conf.*, Sept. 1986, pp. 453–458.
[30] P. Carle, "Multiport branch-waveguide couplers with arbitrary power splitting," in *1989 MTT-S Int. Microwave Symp.* Dig., June 1989, pp. 317–320.
[31] A. Woode and J. Petit, "Investigations into multipactor breakdown in satellite microwave payloads," *ESA Journal*, vol. 14, pp. 467–478, 1990.

Jaime Esteban was born in Madrid, Spain, in 1963. He received the Ingeniero de Telecommunicación and Ph.D. degrees from the Universidad Politécnica de Madrid, Spain, in September 1987 and July 1990, respectively.

From January 1988 to October 1990 he was with the Grupo de Electromagnetismo Aplicado y Microondas at the Universidad Politécnica de Madrid working on numerical methods for electromagnetism with a scholarship from the Spanish Ministry of Education and Science. He is currently Assistant Professor in the Departamento de Electromagnetismo y Teoría de Circuitos, Universidad Politécnica de Madrid. His research interests include the analysis and design of microwave and millimeter-wave devices and the analysis and characterization of waveguides and transmission lines.

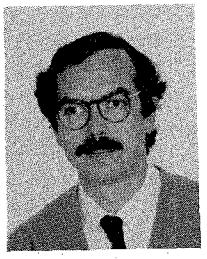

Jesús M. Rebollar was born in Beasain (Guipuzcoa), Spain, in 1953. He received the Ingeniero de Telecomunicación degree in 1975 and the Ph.D. degree in 1980, both from the Universidad Politécnica de Madrid, Spain.

Since 1976 he has been with the Grupo de Electromagnetismo Aplicado y Microondas at the Universidad Politécnica de Madrid as Assistant Professor (1977–1982) and Associate Professor (1982–1988). In 1988, he was appointed Professor of Teoría Electromagnética.

His current research interests include electromagnetic wave propagation in waveguide structures, interactions of electromagnetic fields with biological tissues, and computer-aided design for microwave and millimeter-wave passive devices.